ACS APPLIED BIO MATERIALS

www.acsabm.org Article

Osteogenic Differentiation of Human Mesenchymal Stem Cells by the Single Action of Luminescent Polyurea Oxide Biodendrimers

Rita F. Pires, João Conde,* and Vasco D. B. Bonifácio*

Cite This: *ACS Appl. Bio Mater.* 2020, 3, 9101−9108 Read Online

ACCESS | Metrics & More | Article Recommendations | Supporting Information

ABSTRACT: Polyurea oxide (PURO) biodendrimers are a class of dendrimers that can trigger osteogenic differentiation of human mesenchymal stem cells (hMSCs). PURO biodendrimers are prepared by simple, solventless oxidation of polyurea dendrimers using hydrogen peroxide as the oxidant in quantitative yield, retaining both biocompatibility (up to 10 mg/mL for higher generations) and the non-traditional intrinsic luminescence. The effect of PURO biodendrimers in the differentiation of hMSCs was found by the single addition to a standard growth medium for MSCs differentiation (without differentiation inducers). After 21 days of incubation, the formation of osteoblasts was confirmed by the alizarin red staining assay and alkaline phosphatase activity. This is the first report of *in vitro* osteodifferentiation fully regulated by synthetic soft polymers such as dendrimers. Current osteogenic differentiation protocols rely on an *in vitro* inducing formulation (including dexamethasone, ascorbic acid, and β-glycerophosphate), which lacks therapeutic potential *in vivo*. The outstanding role of dendrimers in nanomedicine, under clinic translation, combined with this feature is envisaged to foster PURO dendrimers as an important strategy in cell therapy and regenerative medicine.

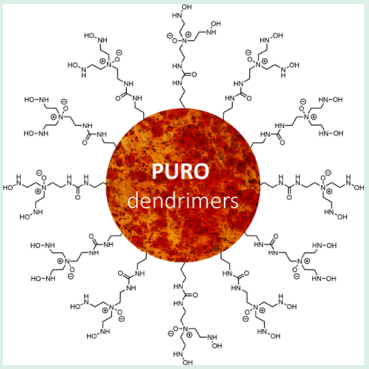

KEYWORDS: *polyurea dendrimers, polyurea oxide dendrimers, green chemistry, human mesenchymal stem cells, osteogenic differentiation*

INTRODUCTION

Human mesenchymal stem cells (hMSCs) have a well-defined differentiation potential, and this ability to differentiate into progenies of multiple lineages is an extraordinary feature that holds a great promise for cell therapy.[1,2] Metabolic changes during the differentiation process show a dramatic decrease of intracellular reactive oxygen species (ROS) as a consequence of upregulation of two antioxidant enzymes, manganese dependent superoxide dismutase and catalase. Reversibly, exogenous hydrogen peroxide (H_2O_2) and mitochondrial inhibitors were found to retard osteogenic differentiation.[3] These findings point toward the mitochondria and ROS key role throughout the differentiation process, giving novel insights for the optimization of *in vitro* differentiation protocols.

The first differentiation to be identified was the mesenchymal stem cell (MSC) osteogenic differentiation.[4,5] This lengthy process (~3 weeks), due to downregulation of DNA by the second week, typically entangles the expression of osteoblast markers such as alkaline phosphatase (ALP), the processing of type I procollagen to collagen I under the effect of ascorbic acid, and the progressive secretion of a collagenous extracellular matrix (ECM), an essential element for the osteogenic differentiation, containing growth factors and many proteins.[6] Hydroxyapatite (HA) deposits mark the final phase of osteoblast phenotypic development.[7] The current protocols for MSCs osteogenic differentiation do not vary significantly and rely on commercial kits. These, however, only provide a routine (control) differentiation protocol that do not translate for tissue engineering and cell-based therapeutics, being alternative strategies for stem cell osteogenic differentiation still on focus.[8]

The combination of stem cells and nanomaterials is a thrilling research field, and in this regard, synthetic polymers such as dendrimers may play a central role. Dendrimers are an extraordinary class of polymers, which unique properties and versatility are mainly due to a well-defined and highly structured layered three-dimensional architecture combined with unlimited surface decoration.[9] A study on the effects of poly(amidoamine) (PAMAM) dendrimers (amino, hydroxyl, and carboxylate surface) on the viability and differentiation ability toward the osteogenic and adipogenic lineages of hMSCs was already reported.[10] Interestingly, despite a concentration-dependent induced cytotoxicity, hMSCs differentiation is not affected by the presence of PAMAM dendrimers.

Received: October 13, 2020
Accepted: November 18, 2020
Published: December 1, 2020

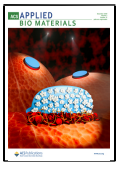

https://dx.doi.org/10.1021/acsabm.0c01315
ACS Appl. Bio Mater. 2020, 3, 9101−9108

Scheme 1. Synthesis of Polyurea Oxide (PURO) Biodendrimers by Oxidation of Polyurea (PURE) Dendrimers: Chemical Structure of Tris(2-aminoethyl)amine oxide (TRENO), Amine Model Compound (a), Schematic Synthesis of PURO Dendrimers from PURE Dendrimers (b), Pictures of PURE Dendrimers after Addition of H_2O_2, and PURO Dendrimers at the End of the Reaction (c)

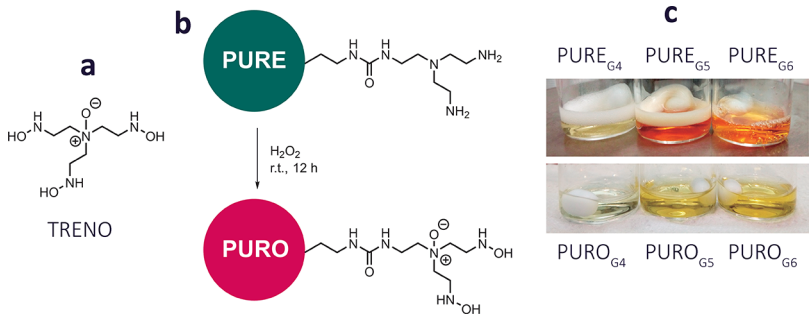

Dendrimer post-functionalization has been extensively explored in biomedical applications and typically restricted to the surface, thus allowing toxicity reduction (*e.g.*, PEGylation, although with some limitations[11]), drug delivery efficacy (*e.g.*, POxylation[12,13]), targeting, labeling and radiolabeling,[14] drug conjugation, or immunomodulation.[15] The (hindering) architecture and (low) monomer reactivity (*e.g.*, amides in PAMAM) may justify branch chemistry postponing. Nevertheless, very recently, we reported the conversion of poly(urea amidoamidine) (PURAM) dendrimers to the corresponding poly(imidazolone amine) (PIMAM) dendrimers, taking advantage of the urea reactivity toward benzoins.[16] Branch modification and simple further *N*-oxidation to poly(imidazolone amine oxide) (PIMAMO) demonstrate the potential of polyurea-based dendrimers as intermediates for architectures with novel functions.

Polyurea (PURE) dendrimers[17] are a class of biocompatible and biodegradable[18] polymers that has shown a pH-dependent non-traditional intrinsic luminescence (NTIL), an unusual property also found in similar systems.[19] PURE dendrimers have a backbone mainly composed of tertiary amines and urea groups, and its surface is layered with primary amines. It is well known that amines are prone to chemical oxidation, even with molecular oxygen from air. In the presence of peroxides, stable nitroxides are formed.[20] The oxidation of branched polyethylene amine (b-PEI) by H_2O_2 was previously reported.[21] In its composition, b-PEI has tertiary, secondary, and primary amines groups, and its oxidation results in the formation of *N*-oxides (from tertiary amines), amides (from secondary amines, in a sequence of dialkylhydroxylamine, nitrone, and oxaziridine intermediates that result in a final Beckmann-type rearrangement), and monoalkylhydroxylamines (from primary amines).

RESULTS AND DISCUSSION

Herein, we investigated the oxidation of PURE dendrimers, containing tertiary amines and ureas in the core and primary amines in the surface using H_2O_2 as the oxidant. Tris(2-aminoethyl)amine (TREN), the monomer used in the synthesis of PURE dendrimers was first used as a model amine, leading to the formation of tris(2-aminoethyl)amine oxide (TRENO) (Scheme 1a). The reaction is very clean and proceeds quantitively. A *meta*-chloroperbenzoic acid (*m*-CPBA)-mediated oxidation was also attempted but a complex mixture was obtained under these conditions. The reaction was then applied to the synthesis of polyurea oxide (PURO) biodendrimers (Scheme 1b). The reaction takes place at room temperature by the simple dropwise addition of a 35% w/w H_2O_2 solution to neat PURE dendrimers. The reaction is highly exothermic and accompanied by gas evolution (Scheme 1c).

After the addition of H_2O_2, PURE dendrimers initially with a brownish orange color (depending on the generation) turned to a light yellow yellowish color after being left under stirring overnight at room temperature. After dilution with water and dialysis, almost colorless oils were obtained. The products were found to be stable for more than 6 months under storage in the fridge (T = 4 °C). At room temperature, after a few weeks, PURO biodendrimers decomposed into dark brown oils.

In the oxidation of PURE dendrimers by H_2O_2, we observed the formation of *N*-oxides and monoalkylhydroxylamines from the oxidation of the tertiary and the primary amines, respectively. FT-IR spectra show a strong band from hydroxylamine and urea groups (νN-OH, NH_{urea}) ~3275 cm^{-1} (Figure 1a) and the characteristic weak band from the *N*-oxide (νN→O) at 950 cm^{-1}.[22] The carbonyl from the urea groups ($\nu C{=}O_{urea}$) is also present at 1645 cm^{-1} (Figure 1b). The oxidation of the urea nitrogen in PURE dendrimers leading to polyhydroxyureas was discarded since ureas are well known to undergo the formation of adducts with hydrogen peroxide (*e.g.*, urea-hydrogen peroxide complex, UHP[23]), releasing hydrogen peroxide in contact with water. The same profile was found for TREN oxidation (Figure S1 in the Supporting Information). ^1H and ^{13}C NMR spectra also corroborate these oxidations. Large downfield chemical shifts (~1 ppm) are observed in all ^1H (Figure 1c) and ^{13}C spectra (Figures S2 and S3 in the Supporting Information).

PURE dendrimers have a pH-dependent blue fluorescence. The fluorescence of dendrimers and other polymers without possessing classic chromophores, referred as a NTIL, has been widely observed and reported.[24−26] Similar to its counterparts, PURO biodendrimers also show a blue fluorescence. However, the emission intensity is higher and permanent, not being influenced by pH changes (both in intensity and emission wavelength). This observation may be easily explained by the formation of *N*-oxides, which local charge leads to repulsion between the dendrimer branches, resulting probably in a more extended and organized conformation. This behavior corresponds to the similar effect of *N*-protonation at low pH (acidification), which we previously reported for PURE dendrimers, where an increasing of the fluorescence emission was observed for pH decreasing. Figure 2 shows the fluorescence spectra of PURO biodendrimers dissolved in

https://dx.doi.org/10.1021/acsabm.0c01315
ACS Appl. Bio Mater. 2020, 3, 9101−9108

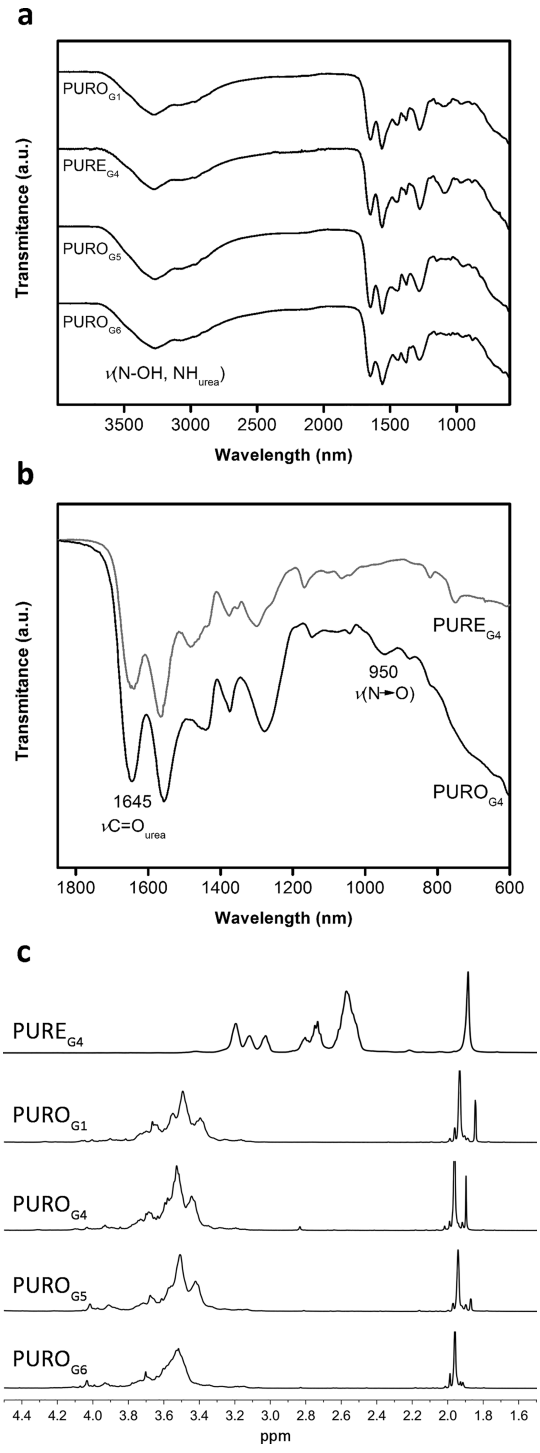

Figure 1. FT-IR and ^{1}H NMR spectra of PURO biodendrimers: FT-IR spectra of PURO biodendrimers (a), comparison of FT-IR spectra of PURE$_{G4}$ and PURO$_{G4}$ (b), and ^{1}H NMR of PURE$_{G4}$ and PURO biodendrimers showing a large downfield chemical shift upon oxidation (c).

distilled water (after dissolution the pH of the solution is 6). To discard the formation of radical species, electron paramagnetic resonance (EPR) spectra were recorded for all PURO biodendrimers but no signals were detected (data not shown).

Regarding oxidative stress, the glutathione *S*-transferase (GST) activity assay showed that PURO biodendrimers no not

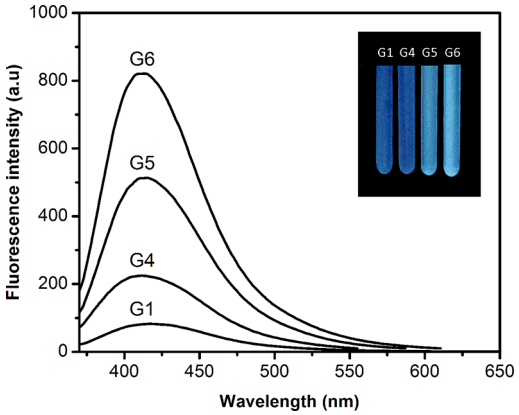

Figure 2. Fluorescence spectra of PURO biodendrimers, generations G_1 to G_6, in water (λ_{ex} = 325 nm). The inset shows a picture of PURO biodendrimers in NMR tubes under UV light (λ_{ex} = 365 nm).

cause glutathione depletion, and thus no oxidative damage was found, even for high concentrations. However, a different behavior was observed for TRENO (model compound), which showed ~30−85% reduction in GST activity (Figure 3A). The

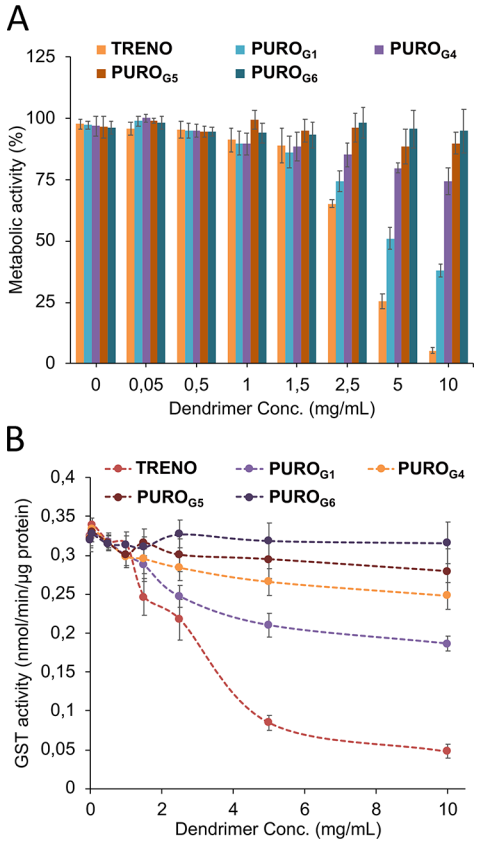

Figure 3. Metabolic activity (A) and GST activity (B) of increasing concentrations of PURO biodendrimers. Data for TRENO is shown for comparison.

[3-(4,5-dimethylthiazol-2-yl-2,5-tetrazolium bromide)] (MTT) assay, revealed that PURO biodendrimers are also highly biocompatible in the studied concentration range, with the exceptions of PURO$_{G1}$ and TRENO for higher concentrations (Figure 3B). In both assays, a correlation

https://dx.doi.org/10.1021/acsabm.0c01315
ACS Appl. Bio Mater. 2020, 3, 9101−9108

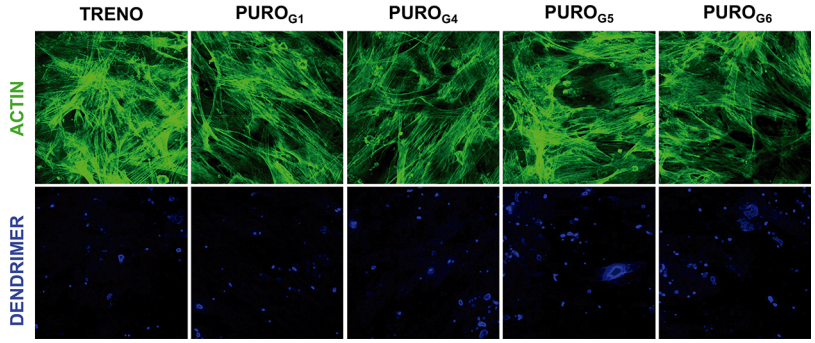

Figure 4. Dendrimers uptake into hMSCs. Confocal microscopy images of hMSCs incubated with TRENO and PURO biodendrimers (1 mg/mL) at 24 h. Top: actin staining by Alexa Fluor 488 phalloidin (λ_{exc} = 495, λ_{em} = 518 nm), a highly selective bicyclic peptide that is used for staining actin filaments (F-actin). Bottom: blue fluorescence from TRENO and PURO biodendrimers.

between oxidative damage, cytotoxicity, and molecular size seems to be present.

To evaluate cellular uptake, confocal microscopy was performed in hMSCs cells treated with TRENO and PURO biodendrimers (1 mg/mL). Both systems have high cellular uptake efficiency at 24 h post-incubation (Figure 4). Confocal imaging showed strong stability of TRENO and PURO biodendrimers and efficient entry into the hMSCs cells, although PURO biodendrimers have higher fluorescence signals, as corroborated in Figure 2. These results clearly demonstrate that both TRENO and PURO biodendrimers exhibit enhanced cellular uptake in hMSCs.

The effect of PURO biodendrimers in the differentiation of hMSCs was investigated. Surprisingly, we found that the single addition of PURO biodendrimers to the standard growth medium for MSCs differentiation[27] (DMEM, Dulbecco's modified Eagle's medium; 10% FBS, fetal bovine serum; 1% glutamine; and 1% penicillin/streptomycin), but excluding dexamethasone, ascorbic acid, and β-glycerophosphate differentiation inducers,[28] triggered an osteogenic differentiation. The formation of osteoblasts was confirmed by performing the alizarin red staining assay and following the alkaline phosphatase (ALP) activity for 21 days (Figure 5). Osteogenesis can be determined by staining with alizarin red solution, which can be used to visually detect the presence of mineralization in bone tissue, by the formation of calcium deposits (stained in red).[29] The ALP assay is the most widely recognized biochemical marker for osteoblast activity. This assay provides a sensitive and a reproducible method that is ideally suited for measuring ALP activity in isolated osteoblastic cells.[30] The osteodifferentiation was found to be proportional to the size of the dendrimer, increasing with increasing molecular weight. Both calcium deposits formation (via alizarin red) and ALP activity of the hMSCs was notably higher in PURO$_{G6}$ if compared with TRENO.

To the best of our knowledge, this is the first report of *in vitro* osteodifferentiation fully regulated by synthetic soft polymers, an envisaged potential.[31] A recent study reported enhanced and accelerated osteogenic differentiation of hMSCs by the synergic effect of osteocalcin/osteopontin (OCN/OPN)-enriched collagen gels, but used in combination with a commercial osteogenic differentiation medium.[32] This OCN-OPN synergy has been attributed to a strong binding of OCN with HA (via γ-carboxyglutamate residues, calcium binding pocket), which is also able to complex *in vitro* with collagen via OPN.[33]

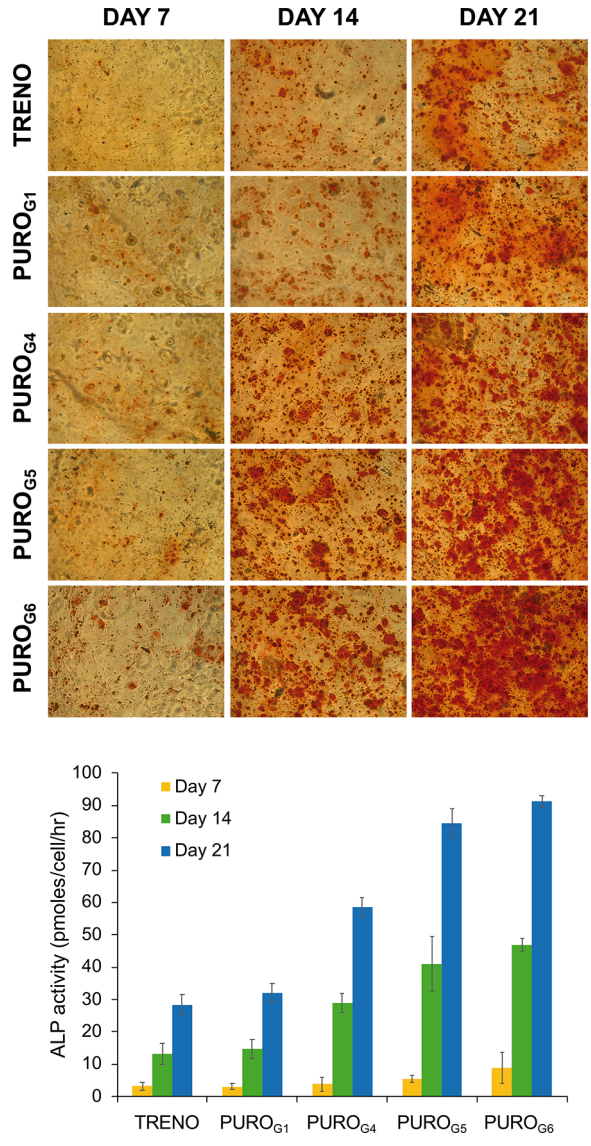

Figure 5. Alizarin red staining (top) and alkaline phosphatase (ALP) activity assay (bottom) for PURO biodendrimers (1 mg/mL) after 7, 14, and 21 days. Alizarin red staining of mineralization in hMSCs during osteogenic differentiation (×100). ALP is used as a marker for human embryonic stem cells.

Nucleation and growth of HA crystals within the collagenous matrix are key steps in bone mineralization,

https://dx.doi.org/10.1021/acsabm.0c01315
ACS Appl. Bio Mater. 2020, 3, 9101−9108

which occurs in the final phase of the osteoblast development. This process is usually assisted by ascorbate and β-glycerophosphate after 2 weeks of culture, when alkaline phosphatase and matrix accumulation is maximal, and both act synergistically to further stimulate alkaline phosphatase activity in differentiated cultures.[7] The mechanism for mineralization enhancement has been postulated to involve a release of inorganic phosphate from β-glycerophosphate catabolism. However, our data show that osteodifferentiation occurs efficiently in β-glycerophosphate free-media, pointing toward other mineralization pathways.

In fact, it has been demonstrated that hMSCs cultured on mineralized matrices in a growth medium, lacking any osteogenic-inducing soluble factors (as in our study), consistently upregulated OPN and OCN.[34] A significant increase in intracellular adenosine triphosphate (ATP) was observed under these conditions, which is obvious since inorganic phosphate is a substrate for ATP synthesis. Also, supplementation of adenosine in a growth medium promoted osteogenic differentiation of hMSCs on nonmineralized matrices, and later found that single adenosine supplementation is also able to induce differentiation of human induced pluripotent stem cell (hiPSC) into functional osteoblasts.[35,36]

These results highlighting the role of phosphate metabolism and adenosine signaling, correlate well with the effect of dexamethasone supplementation. Dexamethasone is a synthetic glucocorticoid, and like other natural glucocorticoids present in FBS, accelerates the upregulation of postproliferative osteoblast phenotype genes. Other components present in FBS, such as retinoic acid and insulin, also showed differentiation promoting properties on osteoblasts.[37] The osteodifferentiation is accompanied with an increase in ATP pools and there is a sharp increase in the glycolysis rate at the latter stage of differentiation,[38] which highlight the importance of glucocorticoids in the regulation of glucose metabolism.

Interestingly, hydroxyurea is known to upregulate ALP and OPN, but without effects on OCN.[39] In contrast, urea is reported to inhibit ALP in human bone tissues extracts, even at low concentrations.[40] PURO biodendrimers lack of hydroxyureas in the backbone (as explained before), and based on our observations, the high content of *N*-substituted urea do not produce any effect on ALP expression (Figure 6). This means that *N*-oxides and terminal *N*-substituted hydroxylamines must play a central role in the observed osteodifferentiation. Previous studies have shown that trimethylamine *N*-oxide (TMAO), which is the structural unit present in PURO biodendrimers, functions as a protein-stabilizing osmolyte, with surfactant properties, and prevent the hydrophobic collapse of elastin-like polypeptides (ELPs),[41] which gels display osteoinductive effects and are promising hMSC high-performance matrices.[42] The properties of TMAO could explain in part the positive effect of PURO biodendrimers on osteodifferentiation, possibly by collagen stabilization. Also, inorganic phosphate and calcium salting-out by *N*-oxides cannot be ruled out as a driving force for HA formation in the mineralization process (Figure 6). Actually, surfactant-assisted HA synthesis proceeds via micelles containing phosphate groups that act as a template to attract calcium.[43] Another interesting feature of PURO biodendrimers is a hydroxylamine-terminated surface. Hydroxylamine is longer known to be a source of free diffusible NO by the action of catalase,[44] and it was already demonstrated that an increase in NO production is parallel to the enhancement of ALP activity, being NO a positive regulator of ALP activity.[45] Thus, NO signaling cannot be ruled out (Figure 6).

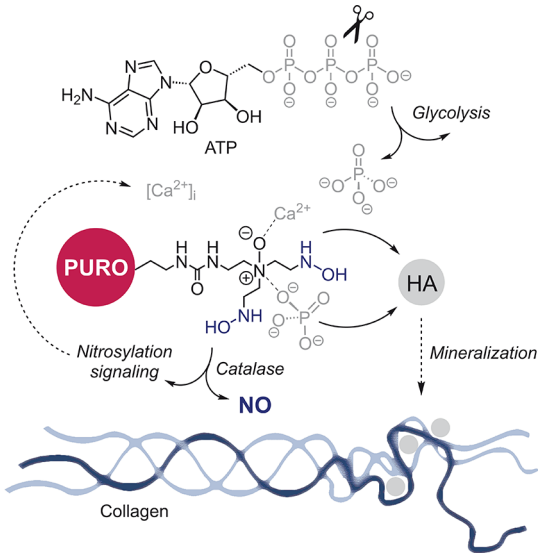

Figure 6. PURO-assisted osteogenic differentiation of human mesenchymal stem cells. PURO, polyurea oxide dendrimer; HA, hydroxyapatite; ATP, adenosine triphosphate; and NO, nitric oxide.

Also, and in a therapeutic perspective, we know that in the human body, triethylamine oxide (TEAO) is reduced into triethylamine (TEA) within the gastrointestinal tract. Experiments indicate that TEAO is fully excreted into the urine in a 24 h period not only by glomerular filtration but also by tubular secretion.[46] Therefore, it is expected that *in vivo* PURO biodendrimers may be also reduced to parent (also non cytotoxic and biocompatible) PURE dendrimers.

CONCLUSIONS

PURO biodendrimers (generations 1 and 4 to 6) were synthesised by simple oxidation of neat PURE biodendrimers using hydrogen peroxide. PURO biodendrimers retained the biocompatibility and blue luminescence of PURE dendrimers and were found to trigger the osteogenic differentiation of human mesenchymal stem cells without the addition of differentiation inducers. PURO biodendrimers are envisaged as potential therapeutics in cell therapy and regenerative medicine.

EXPERIMENTAL SECTION

PURO Synthesis. PURE dendrimers were synthesized using our supercritical CO_2-assisted polymerization protocol.[17] A hydrogen peroxide 35% w/w solution (1 mL) was carefully added dropwise to neat PURE dendrimers (100 mg) at room temperature, over ∼15 min. Upon each drop addition, an intense reaction is observed with strong gas evolution and temperature increase. A discoloration of the solution is also observed from amber to light brown. The reaction was allowed to proceed overnight under stirring. After this period hydrogen peroxide is removed in a rotavapor and the residue diluted with water and dialyzed for ∼24 h. The dialysis is finished after a negative test for hydrogen peroxide in the dialysate water using QUANTOFIX peroxide test strips.

TRENO. FT-IR (neat) ν (cm^{-1}): 3238, 1655, 1575, 1384, 1386, 1240, 948, 878. UV−Vis: λ_{max} = 325 nm (H_2O). Fluorescence (H_2O, λ_{ex} = 325 nm): λ_{em} = 420 nm. ^1H NMR (400 MHz, D_2O) δ (ppm): 3.30−3.24 (m, 3H), 3.02−2.94 (m, 3H), 2.74 (t, J = 6.8 Hz, 3H), 2.55 (dd, J = 7.6, 6.1 Hz, 3H). ^{13}C NMR (100.9 MHz, D_2O) δ

https://dx.doi.org/10.1021/acsabm.0c01315
ACS Appl. Bio Mater. 2020, 3, 9101−9108

(ppm): 164.47, 163.96, 68.37, 66.95, 65.53, 56.62, 55.32, 53.98, 39.03, 37.68, 36.34, 35.99, 34.63, 33.26.

PURO$_{G1}$. FT-IR (neat) ν (cm^{-1}): 3278, 1652, 1558, 1278, 1100, 965. UV−Vis: λ_{max} = 350 nm (H_2O). Fluorescence (H_2O, λ_{ex} = 350 nm): λ_{em} = 417 nm. ^1H NMR (400 MHz, D_2O) δ (ppm): 4.03−3.27 (m), 1.93 (s), 1.84 (s). ^{13}C NMR (100.9 MHz, D_2O) δ (ppm): 181.15, 176.74, 174.37, 174.27, 173.81, 170.83, 164.46, 159.84, 159.65, 64.72, 64.66, 63.86, 63.80, 61.12, 60.55, 60.50, 43.28, 34.74, 34.55, 34.18, 33.56, 33.50, 32.19, 32.13, 23.25, 21.81.

PURO$_{G4}$. FT-IR (neat) ν (cm^{-1}): 3280, 1652, 1564, 1276, 954. UV−Vis: λ_{max} = 350 nm (H_2O). Fluorescence (H_2O, λ_{ex} = 350 nm): λ_{em} = 412 nm. ^1H NMR (400 MHz, D_2O) δ (ppm): 4.02−3.28 (m), 1.96 (s), 1.90 (s). ^{13}C NMR (100.9 MHz, D_2O) δ (ppm): 180.63, 174.33, 170.82, 164.48, 159.86, 159.65, 64.66, 63.78, 61.07, 60.44, 34.73, 34.54, 34.21, 34.09, 33.83, 33.50, 22.80, 21.76.

PURO$_{G5}$. FT-IR (neat) ν (cm-^{1}): 3277, 1651, 1561, 1280, 944. UV-Vis: λ_{max} = 350 nm (H_2O). Fluorescence (H_2O, λ_{ex} = 350 nm): λ_{em} = 415 nm. ^1H NMR (400 MHz, D_2O) δ (ppm): 4.08−3.32 (m), 1.94 (s). ^{13}C NMR (100.9 MHz, D_2O) δ (ppm): 174.31, 174.21, 170.76, 159.82, 159.62, 64.68, 63.81, 61.08, 60.46, 46.57, 34.78, 34.58, 34.22, 34.11, 33.51, 21.80.

PURO$_{G6}$. FT-IR (neat) ν (cm^{-1}): 3273, 1649, 1565, 1282, 960. UV−Vis: λ_{max} = 350 nm (H_2O). Fluorescence (H_2O, λ_{ex} = 350 nm): λ_{em} = 414 nm. ^1H NMR (400 MHz, D_2O) δ (ppm): 3.58−3.48 (m), 1.96 (s). ^{13}C NMR (100.9 MHz, D_2O) δ (ppm): 176.63, 174.44, 174.39, 174.34, 174.29, 173.85, 170.60, 160.99, 159.85, 159.65, 158.64, 64.75, 64.65, 63.79, 61.09, 60.50, 60.45, 46.60, 43.22, 34.80, 34.59, 34.10, 33.59, 33.47, 21.82.

Cell Culture. Human bone marrow MSCs were purchased from Sigma-Aldrich. The hMSCs were cultured with the osteogenic medium (for cell uptake, MTT, GST oxidative stress, and ALP assay): DMEM, 10%FBS, 1% glutamine, 1% penstrep, 100 nM dexamethasone, 200 μM ascorbic acid, and 10 mM glycerol-2-phospate. For alizarin red assay, the MSCs were cultured with medium: DMEM, no calcium; 10%FBS; 1% glutamine; and 1% penstrep. hMSCs were cultured at 37 °C in a humidified atmosphere containing 95% air and 5% CO_2. The confluent cells were passaged with 0.25% trypsin for up to 3 passages.

Glutathione *S*-Transferase (GST) Activity Assay. After 48 h treatment with increasing concentrations of TRENO and PURO dendrimers, cells were washed with 1× PBS (phosphate-buffered saline), lysed in ultrapure water and the pellets resuspended in 50 mL ultrapure water. Briefly, GST activity was determined based on a described protocol,[47] by measuring the conjugation of 1-chloro-2,4-dinitrobenzene with glutathione (GSH). The enzyme activity was determined by measuring the absorbance at every minute during a maximum of 10 min on a 96-well plate, using three replicas for each sample. The change in absorbance was measured at 340 nm using a microplate reader and values were normalized to total protein concentration determined by the Bradford assay (Thermo Scientific).

Metabolic Activity by MTT Assay. Standard MTT [3-(4,5-dimethylthiazol-2-yl)-2,5-diphenyltetrazoliumbromide] reduction assay (Invitrogen) was performed to determine the cytotoxicity of both TRENO and PURO dendrimers. Briefly, cells were seeded at a density of 1×10^5 cells per well in 24-well culture plates in complete DMEM (500 mL) with serum. After 48 h treatment with increasing concentrations (0.05, 0.5, 1, 1.5, 2.5, 5, and 10 mg/mL) of TRENO and PURO dendrimers, medium was then removed, and cells were washed two times with sterile PBS and 300 mL of a fresh medium with serum was added. For the assay, 16.7 μL of sterile MTT stock solution (5 mg/mL in PBS) were added to each well, incubated for 2 h, the medium removed, and the formazan crystals resuspended in 300 mL of dimethyl sulfoxide (DMSO from Sigma). The solution was mixed, and its absorbance was measured at 540 nm as the working wavelength and 630 nm as the reference using a microplate reader. The cell viability was normalized to that of cells cultured in the culture medium with PBS treatment. The experiments were repeated three times.

Alizarin Red Staining. Osteogenic differentiation was confirmed by alizarin red staining on days 7, 14, and 21. Cells were sequentially washed twice with PBS, fixed with 95% ethanol for 20 min, rinsed three times with Mili-Q water, and stained by alizarin red solution (Merck Millipore) for 30 min at 37 °C. After washing four times with Mili-Q water, the stained cells were photographed in a regular optical microscope. Staining was performed in three replicates.

Alkaline Phosphatase (ALP). Reaching 100% confluence, cultured MSC cells were transferred to the osteogenic induction medium. MSC were incubated for 7, 14, and 21 days. The cultured cells were washed two times with PBS and collected in 0.1 M Tris buffer containing 0.1% Triton X-100. Cellular membranes were lysed by a freeze−thaw method in cell lysis solution (0.2% Triton X-100, 10 mM Tris (pH 7.0), and 1 mM EDTA). Aliquots of supernatants were subjected to ALP activity measurement and protein assay according to the Bradford's method. The ALP activity was determined using 50 mM *p*-nitrophenylphosphate in a sodium carbonate buffer at pH 10.4, followed by incubation at 37 °C for 30 min. After adding 0.2 M NaOH, the amount of released *p*-nitrophenylphosphate was estimated by measuring the absorbance at 405 nm.

■ ASSOCIATED CONTENT

Supporting Information

The Supporting Information is available free of charge at https://pubs.acs.org/doi/10.1021/acsabm.0c01315.

FT-IR and NMR spectra of TRENO and PURO dendrimers (PDF)

■ AUTHOR INFORMATION

Corresponding Authors

João Conde − *NOVA Medical School, Faculdade de Ciências Médicas and Centre for Toxicogenomics and Human Health (ToxOmics), Genetics, Oncology and Human Toxicology, NOVA Medical School, Faculdade de Ciências Médicas, Universidade Nova de Lisboa, Lisboa 1169-056, Portugal;* orcid.org/0000-0001-8422-6792; Email: joao.conde@nms.ul.pt

Vasco D. B. Bonifácio − *iBB-Institute for Bioengineering and Biosciences, Instituto Superior Técnico, Universidade de Lisboa, Lisboa, Lisboa 1049-001, Portugal;* orcid.org/0000-0003-2349-8473; Email: vasco.bonifacio@tecnico.ulisboa.pt

Author

Rita F. Pires − *iBB-Institute for Bioengineering and Biosciences, Instituto Superior Técnico, Universidade de Lisboa, Lisboa, Lisboa 1049-001, Portugal*

Complete contact information is available at: https://pubs.acs.org/10.1021/acsabm.0c01315

Notes

The authors declare no competing financial interest.

■ ACKNOWLEDGMENTS

We thank Fundação para a Ciência e a Tecnologia for financial support through project PTDC/MEC-ONC/29327/2017 and the PhD grant SFRH/BD/109006/2015 (R.F.P.). We also thank Dr. Luisa Maia (UCIBIO, FCT-UNL) for EPR measurements.

■ REFERENCES

(1) Pittenger, M. F.; Discher, D. E.; Péault, B. M.; Phinney, D. G.; Hare, J. M.; Caplan, A. I. Mesenchymal stem cell perspective: Cell biology to clinical progress. *npj Regen. Med.* **2019**, *4*, 22.

(2) Gomez-Salazar, M.; Gonzalez-Galofre, Z. N.; Casamitjana, J.; Crisan, M.; James, A. W.; Péault, B. Five decades later, are

mesenchymal stem cells still relevant? *Front. Bioeng. Biotechnol.* **2020**, *8*, 148.
(3) Chen, C.-T.; Shih, Y.-R. V.; Kuo, T. K.; Lee, O. K.; Wei, Y.-H. Coordinated changes of mitochondrial biogenesis and antioxidant enzymes during osteogenic differentiation of human mesenchymal stem cells. *Stem Cells* **2008**, *26*, 960−968.
(4) Friedenstein, A. J.; Petrakova, K. V.; Kurolesova, A. I.; Frolova, G. P. Heterotopic of bone marrow. Analysis of precursor cells for osteogenic and hematopoietic tissues. *Transplantation* **1968**, *6*, 230−247.
(5) Friedenstein, A. J.; Chailakhjan, R. K.; Lalykina, K. S. The development of fibroblast colonies in monolayer cultures of guinea-pig bone marrow and spleen cells. *Cell Proliferation* **1970**, *3*, 393−403.
(6) El-Amin, S. F.; Lu, H. H.; Khan, Y.; Burems, J.; Mitchell, J.; Tuan, R. S.; Laurencin, C. T. Extracellular matrix production by human osteoblasts cultured on biodegradable polymers applicable for tissue engineering. *Biomaterials* **2003**, *24*, 1213−1221.
(7) Quarles, L. D.; Yohay, D. A.; Lever, L. W.; Caton, R.; Wenstrup, R. J. Distinct proliferative and differentiated stages of murine MC3T3-E1 cells in culture: An in vitro model of osteoblast development. *J. Bone Miner. Res.* **1992**, *7*, 683−692.
(8) Pinheiro, C. C. G.; Bueno, D. F. *Alternative strategies for stem cell osteogenic differentiation in osteogenesis and bone regeneration*; Yang, H. (Ed.), IntechOpen: 2018.
(9) Tomalia, D. A.; Christensen, J. B.; Boas, U. *Dendrimers, dendrons, and dendritic polymers: Discovery, applications, and the future*; Cambridge University Press: New York, 2012.
(10) Goncalves, M.; Castro, R.; Rodrigues, J.; Tomas, H. The effect of PAMAM dendrimers on mesenchymal stem cell viability and differentiation. *Curr. Med. Chem.* **2012**, *19*, 4969−4975.
(11) Thi, T. T. H.; Pilkington, E. H.; Nguyen, D. H.; Lee, J. S.; Park, K. D.; Truong, N. P. The Importance of poly(ethylene glycol) alternatives for overcoming PEG immunogenicity in drug delivery and bioconjugation. *Polymer* **2020**, *12*, 298.
(12) Restani, R. B.; Conde, J.; Pires, R. F.; Martins, P.; Fernandes, A. R.; Baptista, P. V.; Bonifácio, V. D. B.; Aguiar-Ricardo, A. POxylated polyurea dendrimers: Smart core-shell vectors with IC_{50} lowering capacity. *Macromol. Biosci.* **2015**, *15*, 1045−1051.
(13) Restani, R. B.; Pires, R. F.; Baptista, P. V.; Fernandes, A. R.; Casimiro, T.; Bonifácio, V. D. B.; Aguiar-Ricardo, A. Nano-in-micro sildenafil dry powder formulations for the treatment of pulmonary arterial hypertension disorders: The synergic effect of POxylated polyurea dendrimers, PLGA, and cholesterol. *Part. Part. Syst. Charact.* **2020**, *37*, 1900447.
(14) Zhao, L.; Zhu, M.; Li, Y.; Xing, Y.; Zhao, J. Radiolabeled dendrimers for nuclear medicine applications. *Molecules* **2017**, *22*, 1350.
(15) Moura, L. I. F.; Malfanti, A.; Peres, C.; Matos, A. I.; Guegain, E.; Sainz, V.; Zloh, M.; Vicent, M. J.; Florindo, H. F. Functionalized branched polymers: Promising immunomodulatory tools for the treatment of cancer and immune disorders. *Mater. Horiz.* **2019**, *6*, 1956−1973.
(16) Pires, R. F.; Charas, A.; Morgado, J.; Casimiro, T.; Bonifácio, V. D. B. Photodiode-like behavior of jelly dye-sensitized donor-acceptor dendrimers. *J. Appl. Polym. Sci.* **2019**, *137*, 48635.
(17) Restani, R. B.; Morgado, P. I.; Ribeiro, M. P.; Correia, I. J.; Aguiar-Ricardo, A.; Bonifácio, V. D. B. Biocompatible polyurea dendrimers with pH-dependent fluorescence. *Angew. Chem., Int. Ed.* **2012**, *51*, 5162−5165.
(18) Pires, R. F.; Moro, A.; Lourenço, A.; Lima, J. C.; Casimiro, T.; Bonifácio, V. D. B. Molecular weight determination by luminescent chemo−enzymatics. *ChemistrySelect* **2016**, *1*, 6818−6822.
(19) Tomalia, D. A.; Klajnert-Maculewicz, B.; Johnson, K. A.-M.; Brinkman, H. F.; Janaszewska, A.; Hedstrand, D. M. Non-traditional intrinsic luminescence: Inexplicable blue fluorescence observed for dendrimers, macromolecules and small molecular structures lacking traditional/conventional luminophores. *Prog. Polym. Sci.* **2019**, *90*, 35−117.
(20) Walling, C. *Free radicals in solution*; Wiley: New York, p. 595, 1957.
(21) Haas, H. C.; Schuler, N. W.; Macdonald, R. L. Oxidized polyethylenimine. *J. Polym. Sci., Part A-1: Polym. Chem.* **1972**, *10*, 3143−3158.
(22) Bernier, D.; Wefelscheid, U. K.; Woodward, S. Properties, Preparation and synthetic uses of amine *N*-oxides. An update. *Org. Prep. Proced. Int.* **2009**, *41*, 173−210.
(23) Matyáš, R.; Selesovsky, J.; Pelikán, V.; Szala, M.; Cudziło, S.; Trzciński, W. A.; Gozin, M. Explosive properties and thermal stability of urea-hydrogen peroxide adduct. *Propellants, Explos., Pyrotech.* **2017**, *42*, 198−203.
(24) Studzian, M.; Pułaski, Ł.; Tomalia, D. A.; Klajnert-Maculewicz, B. Non-traditional intrinsic luminescence (NTIL): Dynamic quenching demonstrates the presence of two distinct fluorophore types associated with NTIL behavior in pyrrolidone-terminated PAMAM dendrimers. *J. Phys. Chem. C* **2019**, *123*, 18007−18016.
(25) Studzian, M.; Działak, P.; Pułaski, L.; Hedstrand, D. M.; Tomalia, D. A.; Klajnert-Maculewicz, B. Synthesis, internalization and visualization of *N*-(4-carbomethoxy) pyrrolidone terminated PAMAM [G5:G3-TREN] tecto(dendrimers) in mammalian cells. *Molecules* **2020**, *25*, 4406.
(26) Konopka, M.; Janaszewska, A.; Johnson, K. A. M.; Hedstrand, D.; Tomalia, D. A.; Klajnert-Maculewicz, B. Determination of non-traditional intrinsic fluorescence (NTIF) emission sites in 1-(4-carbomethoxypyrrolidone)-PAMAM dendrimers using CNDP-based quenching studies. *J. Nanopart. Res.* **2018**, *20*, 220.
(27) Hagmann, S.; Moradi, B.; Frank, S.; Dreher, T.; Kämmerer, P. W.; Richter, W.; Gotterbarm, T. Different culture media affect growth characteristics, surface marker distribution and chondrogenic differentiation of human bone marrow-derived mesenchymal stromal cells. *BMC Musculoskeletal Disord.* **2013**, *14*, 223.
(28) Coelho, M. J.; Fernandes, M. H. Human bone cell cultures in biocompatibility testing. Part II: Effect of ascorbic acid, β-glycerophosphate and dexamethasone on osteoblastic differentiation. *Biomaterials* **2000**, *21*, 1095−1102.
(29) Gregory, C. A.; Gunn, W. G.; Peister, A.; Prockop, D. J. An Alizarin red-based assay of mineralization by adherent cells in culture: Comparison with cetylpyridinium chloride extraction. *Anal. Biochem.* **2004**, *329*, 77−84.
(30) Sabokbar, A.; Millett, P. J.; Myer, B.; Rushton, N. A rapid, quantitative assay for measuring alkaline phosphatase activity in osteoblastic cells in vitro. *Bone Miner.* **1994**, *27*, 57−67.
(31) Murphy, W. L.; McDevitt, T. C.; Engler, A. J. Materials as stem cell regulators. *Nat. Mater.* **2014**, *13*, 547−557.
(32) Carvalho, M. S.; Poundarik, A. A.; Cabral, J. M. S.; da Silva, C. L.; Vashishth, D. Biomimetic matrices for rapidly forming mineralized bone tissue based on stem cell-mediated osteogenesis. *Sci. Rep.* **2018**, *8*, 14388.
(33) Prince, C. W.; Dickie, D.; Krumdieck, C. L. Osteopontin, a substrate for transglutaminase and Factor XIII activity. *Biochem. Biophys. Res. Commun.* **1991**, *177*, 1205−1210.
(34) Shih, Y.-R. V.; Hwang, Y.; Phadke, A.; Kang, H.; Hwang, N. S.; Caro, E. J.; Nguyen, S.; Siu, M.; Theodorakis, E. A.; Gianneschi, N. C.; Vecchio, K. S.; Chien, S.; Lee, O. K.; Varghese, S. Calcium phosphate-bearing matrices induce osteogenic differentiation of stem cells through adenosine signaling. *Proc. Natl. Acad. Sci. U. S. A.* **2014**, *111*, 990−995.
(35) Kang, H.; Shih, Y.-R. V.; Nakasaki, M.; Kabra, H.; Varghese, S. Small molecule−driven direct conversion of human pluripotent stem cells into functional osteoblasts. *Sci. Adv.* **2016**, *2*, No. e1600691.
(36) Kang, H.; Shih, Y.-R. V.; Varghese, S. Direct conversion of human pluripotent stem cells to osteoblasts with a small molecule. *Curr. Protoc. Stem Cell Biol.* **2018**, *44*, 1F.21.
(37) Lian, J. B.; Stein, G. S. Concepts of osteoblast growth and differentiation: Basis for modulation of bone cell development and tissue formation. *Crit. Rev. Oral Biol. Med.* **1992**, *3*, 269−305.
(38) Komarova, S. V.; Ataullakhanov, F. I.; Globus, R. K. Bioenergetics and mitochondrial transmembrane potential during

https://dx.doi.org/10.1021/acsabm.0c01315
ACS Appl. Bio Mater. 2020, 3, 9101−9108

differentiation of cultured osteoblasts. *Am. J. Physiol. Cell. Physiol.* **2000**, *279*, C1220−C1229.
(39) Owen, T. A.; Aronow, M.; Shalhoub, V.; Barone, L. M.; Wilming, L.; Tassinari, M. S.; Kennedy, M. B.; Pockwinse, S.; Lian, J. B.; Stein, G. S. Progressive development of the rat osteoblast phenotype in vitro: Reciprocal relationships in expression of genes associated with osteoblast proliferation and differentiation during formation of the bone extracellular matrix. *J. Cell. Physiol.* **1990**, *143*, 420−430.
(40) Bahr, M.; Wilkinson, J. H. Urea as a selective inhibitor of human tissue alkaline phosphatases. *Clin. Chim. Acta* **1967**, *17*, 367−370.
(41) Liao, Y.-T.; Manson, A. C.; DeLyser, M. R.; Noid, W. G.; Cremer, P. S. Trimethylamine *N*-oxide stabilizes proteins via a distinct mechanism compared with betaine and glycine. *Proc. Natl. Acad. Sci. U. S. A.* **2017**, *114*, 2479−2484.
(42) Glassman, M. J.; Avery, R. K.; Khademhosseini, A.; Olsen, B. D. Toughening of thermoresponsive arrested networks of elastin-like polypeptides to engineer cytocompatible tissue scaffolds. *Biomacromolecules* **2016**, *17*, 415−426.
(43) Wang, Y.; Chen, J.; Wei, K.; Zhang, S.; Wang, X. Surfactant-assisted synthesis of hydroxyapatite particles. *Mater. Lett.* **2006**, *60*, 3227−3231.
(44) Nicholls, P. The reactions of azide with catalase and their significance. *Biochem. J.* **1964**, *90*, 331−343.
(45) Orciani, M.; Trubiani, O.; Vignini, A.; Mattioli-Belmonte, M.; Di Primio, R.; Salvolini, E. Nitric oxide production during the osteogenic differentiation of human periodontal ligament mesenchymal stem cells. *Acta Histochem.* **2009**, *111*, 15−24.
(46) Åkesson, B.; Vinge, E.; Skerfving, S. Pharmacokinetics of triethylamine and triethylamine-*N*-oxide in man. *Toxicol. Appl. Pharmacol.* **1989**, *100*, 529−538.
(47) Habig, W. H.; Pabst, M. J.; Jakoby, W. B. Glutathione S-transferases. The first enzymatic step in mercapturic acid formation. *J. Biol. Chem.* **1974**, *249*, 7130−7139.

https://dx.doi.org/10.1021/acsabm.0c01315
ACS Appl. Bio Mater. 2020, 3, 9101−9108